Korean J. Chem. Eng., **26**(5), 1291-1295 (2009)
DOI: 10.1007/s11814-009-0203-x

The effect of metal ions in MNaY-zeolites for the adsorptive removal of tetrahydrothiophene

Yun Ha Kim*, Hee Chul Woo, Doohwan Lee***, Hyun Chul Lee***, and Eun Duck Park*,†**

*Division of Energy Systems Research and Division of Chemical Engineering and Materials Engineering, Ajou University, Wonchun-dong Yeongtong-gu, Suwon 443-749, Korea
**Division of Applied Chemical Engineering, Pukyong National University, San 100 Yongdang-dong, Nam-gu, Busan 608-739, Korea
***Energy and Environment Laboratory, Samsung Advanced Institute of Technology (SAIT), P.O. Box 111, Suwon 440-600, Korea
(*Received 6 November 2008 • accepted 10 February 2009*)

Abstract−The adsorptive removal of tetrahydrothiophene (THT) was carried out over transition metal ion-exchanged Na-Y zeolites. CuNa-Y, CoNa-Y, NiNa-Y and FeNa-Y were prepared by a conventional ion exchange method from Na-Y using the nitrate solutions of corresponding metals. N_2 physisorption, inductively coupled plasma-atomic emission spectroscopy (ICP-AES) and X-ray diffraction were conducted to characterize adsorbents. The temperature programmed desorption (TPD) of THT was also perfomed to probe the interaction between the adsorbent and the THT. The crystal structure of Y-zeolite was completely destroyed in FeNa-Y, which resulted in a insignificant amount of adsorbed THT. The breakthrough capacity, which is defined as the amount of sulfur adsorbed on the adsorbent before detecting sulfur species by PFPD, decreased in the following order CuNa-Y>CoNa-Y>NiNa-Y≫FeNa-Y. For interaction between THT and adsorbent, a TPD peak appeared over CoNa-Y at the highest temperature, which implies that the strongest interaction can be made between THT and Co^{2+} in CoNa-Y.

Key words: Adsorption, Tetrahydrothiophene, Zeolite, Ion-exchange, Fuel Cell

INTRODUCTION

Natural gas (NG) can be a promising hydrogen source for fuel cell applications because it is abundant in nature and easy to deliver as a city gas through well-distributed pipeline networks. Generally, the city gas contains organic sulfur compounds such as *tert*-butylmercaptan (TBM), dimethylsulfide (DMS) and tetrahydrothiophene (THT) as odorants for detecting leakage of the gas. These organic sulfur compounds should be removed for natural gas to be used as a hydrogen source for the fuel cell because they can irreversibly deactivate fuel processing catalysts and fuel cell electrodes [1,2]. Among various desulfurization methods, the adsorptive removal of sulfur species from fuels has been widely investigated because this can be more effective for the small-scale process compared with the conventional hydrodesulfurization (HDS) [3,4]. The former system can be operated at low temperatures and pressures without additional hydrogen supply [5,6].

Until now, the adsorptive removal of sulfur species has been carried out over various adsorbents such as porous carbon materials [7], metal impregnated oxides [8], X zeolite [9-11], ZSM-5 [12], β-zeolite (BEA) [13-15], and Y-zeolite [16-22]. Among them, β-zeolite and the ultra stable Y-zeolite (USY) have been reported to offer particularly high adsorption capacity [23]. In the case of BEA, it was reported that the addition of metal could increase the adsorption capacity of sulfur compound [14,15]. Among Y zeolites, Ag-Y and Cu-Y zeolites have been reported to offer high adsorption capacity for thiophene and its derivatives via specific π-interactions [3,17]. Previous studies have focused on the adsorptive removal of sulfur odorants using Ag-Y zeolites [20-22].

Among organic sulfur compounds, comparatively fewer works have been reported on the adsorptive removal of THT compared with those on TBM or DMS [6,11,13-15,22-29]. Furthermore, no relevant work has been conducted on the interaction between THT and the adsorption sites in metal-ion-exchanged Y zeolites. In this study, we prepared some transition metal-ion-exchanged Na-Y adsorbents and examined the adsorption and desorption characteristics of THT.

EXPERIMENTAL

A powder form of Na-Y zeolite (320NAA, Tosoh Co., Japan, the molar ratio of Si/Al=2.81) was used as the precursor for metal ion-exchanged Y (MNa-Y) zeolites. Na-Y zeolite was pretreated at 773 K for 3 h with dry air. $Cu(NO_3)_2$ (Aldrich, 99.9%), $Co(NO_3)_2$ (Junsei, 98%), $Ni(NO_3)_2$ (Junsei, 97%), and $Fe(NO_3)_3$ (Junsei, 98%) were dissolved into deionized water for its concentration to be 0.1 M. Then Na-Y zeolite was added in these solutions (15 ml solution/g Na-Y), and kept at 333 K for 3 h with stirring. After an ion-exchange procedure, the slurry containing MNa-Y was filtered and MNa-Y was rinsed with the deionized water several times and dried at 383 K overnight. Finally, MNa-Y zeolites were pretreated at 773 K for 4 h with dry air.

The surface area of Na-Y and MNa-Y was analyzed with an Autosorb-1 apparatus (Quantachrome) at liquid N_2 temperature. Before analysis, the sample was vacuum treated at 473 K for 2 h. The

†To whom correspondence should be addressed.
E-mail: edpark@ajou.ac.kr

specific micropore volume was determined by the *t*-plot method [30].

The composition of the ion-exchanged samples was analyzed by inductively coupled plasma-atomic emission spectroscopy (ICP-AES, JY-70Plus, Jobin-Yvon). Temperature programmed desorption (TPD) of THT adsorbed on the adsorbents was conducted over 30 mg of sample at a heating rate of 10 K/min monitoring thermal conductivity detector (TCD) and mass signals using an AutoChem 2910 unit (Micromeritics) and a mass spectrometer (QMS 200, Pfeiffer Vacuum), respectively, after THT was loaded on the adsorbent at 313 K by a pulse injection. XRD patterns were obtained by using Cu Kα radiation (λ=1.5406 Å) with a Rigaku D/MAC-III instrument at room temperature.

Sulfur uptake on the adsorbents was measured at 303 K and atmospheric pressure by using a small fixed bed reactor with adsorbents. A feed gas of 100 ppm THT balanced with CH_4 was fed to the reactor, in which 0.10 g of adsorbents was charged, at a flow rate of 55 ml/min. Before the sulfur uptake measurements, all the adsorbents were pretreated at 773 K for 1 h with dry air. The effluent from the reactor was analyzed by gas chromatograph (Donam, DS6100) with a pulsed flame photometric detector (PFPD) and a flame ionization detector (FID). The breakthrough uptake was defined as the amount of sulfur adsorbed on the adsorbent before detecting sulfur species by PFPD (the lower detection limit of PFPD=~50 ppb S). The total uptake was calculated by the following formula:

$$\text{total sulfur uptake} = \frac{F}{M}\int_0^t (C_{in} - C_{ef})dt.$$

In this equation, F is the molar flow rate of the feed, M is the weight of the adsorbent, C_{in} is the sulfur concentration in the feed, C_{ef} is the sulfur concentration in the effluent, and t is the time.

RESULTS AND DISCUSSION

Table 1 shows the physical properties of the parent Na-Y and metal ion-exchanged MNa-Y. The molar ratio of metal ions to aluminum in the sample increased in the following order: CuNa-Y< CoNa-Y<NiNa-Y. This implies that the ion-exchangeability of ions increases in the same order. The total concentration of ions considering the divalent nature of transition metal ions such as Cu^{2+}, Co^{2+}, and Ni^{2+} was determined to be almost same with the concentration of aluminum metal in the sample, which can support that all the metal ions are present in the ionic state not metal oxides. On the other hand, larger amounts of Fe^{3+} were determined to be present in FeNa-Y, which corresponded to the double of the quantity calculated based on the assumption that Fe^{3+} and Na^+ can occupy the ion-exchangeable site formed by the presence of aluminum in the structure of Y-zeolite. This fact implies that some of Fe species can be present as iron oxides. The molar ratios of SiO_2/Al_2O_3 in CuNa-Y, CoNa-Y, and NiNa-Y were determined to be similar to that of parent Na-Y, which can be interpreted as that the dealumination did not occur during the ion-exchange procedure. On the other hand, the molar ratio of SiO_2/Al_2O_3 in FeNa-Y was determined to be larger than that of parent Na-Y, which implies that dealumination can proceed during the sample preparation. The BET surface areas and the normalized surface areas for Na-Y, CuNa-Y, CoNa-Y and NiNa-Y were determined to be similar to each other. However, much smaller corresponding values were obtained for FeNa-Y. This also strongly supports that the zeolite structure of FeNa-Y is destroyed significantly during the sample preparation. The specific micropore volume decreased in the following order: CuNa-Y>CoNa-Y>NiNa-Y.

The oxidation state of metal species in MNa-Y prepared by the same procedure taken in this work has been well documented. Silver, copper, cobalt, and nickel species in MNa-Y can be present as Ag^+ [31], Cu^{2+} [32], Co^{2+} [33], and Ni^{2+} [34], respectively. In the case of CuNa-Y, the auto reduction from Cu^{2+} to Cu^+ has been reported to occur during heat treatment above 350 °C [35]. Therefore, the oxidation state of copper in CuNa-Y might be +1 after the pretreatment in this work. However, in the case of FeNa-Y, it was reported that the Fe(III) solutions with Na-Y induced precipitation of $Fe(OH)_3$ and disintegration of the zeolite structure [36]. This can be confirmed by XRD patterns as shown in Fig. 1. For all MNa-Y except FeNa-Y, the crystalline structure of Na-Y was maintained after an ion-exchange procedure. However, no characteristic XRD peaks of Y zeolite can be found in FeNa-Y. Therefore, CuNa-Y, CoNa-Y, and NiNa-Y were selected for further studies in this work.

The adsorption characteristics with a feed composed of 100 ppm THT in CH_4 were examined over CuNa-Y, CoNa-Y, and NiNa-Y as shown in Fig. 2. The general adsorption pattern with time on stream can be divided into three steps. At the first step, no detectable THT

Table 1. The physical properties of metal ion-exchanged MNa-Y

Sample	BET surface area (m^2/g)	Normalized surface area[a] (10^3 m^2/g-Al)	Micropore volume (cc/g)	Na/Al (mol/mol)	Metal/Al (mol/mol)	F[b]	SiO_2/Al_2O_3 (mol/mol)
Na-Y	702.4	6.3	0.3208	1.07	0.00	1.00	5.60
CuNa-Y	706.9	6.1	0.3133	0.51	0.24	0.99	5.16
CoNa-Y	707.2	6.1	0.3080	0.43	0.27	0.97	5.13
NiNa-Y	656.0	5.7	0.2920	0.40	0.30	1.00	5.28
FeNa-Y	159.2	1.7	0.0434	0.25	0.57	1.96	6.40

[a]The surface area was normalized with Al content in each sample, $S_{Al}\left(\frac{m^2}{gram-Al}\right) = S\left(\frac{m^2}{gram-sample}\right) \times \frac{gram\ of\ sample}{weight\ of\ Al\ in\ the\ sample}$

[b]The fraction of occupied ion-exchangeable sites calculated by the following formula

$$F = \frac{[Na^+]_{MNa\text{-}Y} + n \times [M^{n+}]_{MNa\text{-}Y}}{[Na^+]_{Na\text{-}Y}}$$

where $[Na^+]_{MNa\text{-}Y}$ and $[M^{n+}]_{MNa\text{-}Y}$ is the concentration of each metal ions in MNa-Y and $[Na^+]_{Na\text{-}Y}$ is the concentration of Na^+ in the parent Na-Y

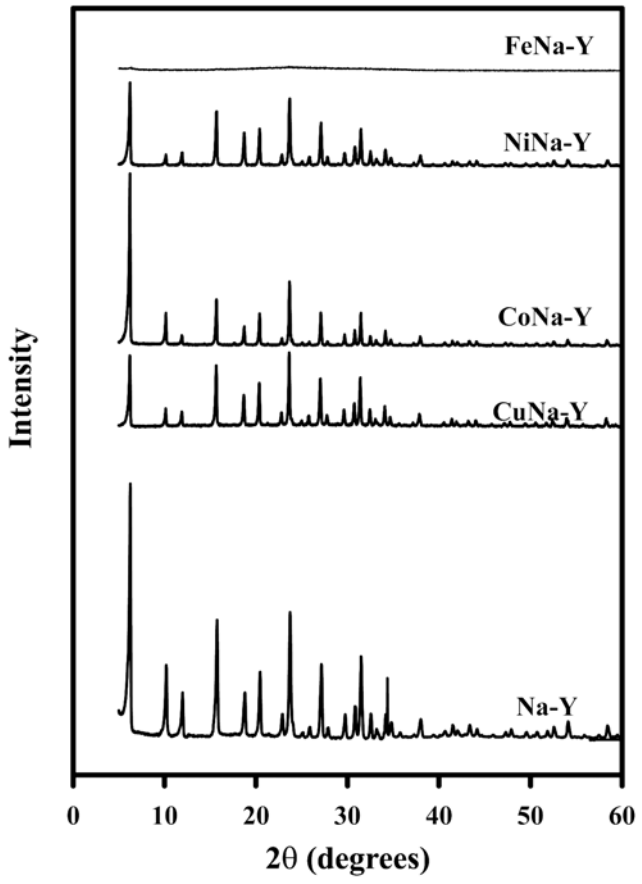

Fig. 1. XRD patterns of Na-Y, CuNa-Y, CoNa-Y, NiNa-Y and Fe Na-Y.

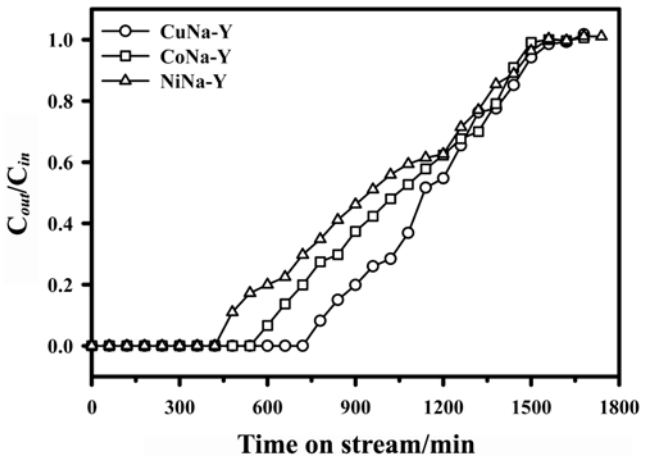

Fig. 2. Concentration profiles of THT in the effluents measured as a function of time during THT adsorption over CuNa-Y, CoNa-Y, and NiNa-Y. The feed gas composed of 100 ppm of THT in CH_4 balance was fed to the reactant with GHSV of 10,000 h^{-1}.

was found in the effluent stream. After a while, THT could be detected in the effluent stream and its concentration increased with time on stream, and finally the THT concentration in the exit reached the same concentration in a feed and was maintained. The time when

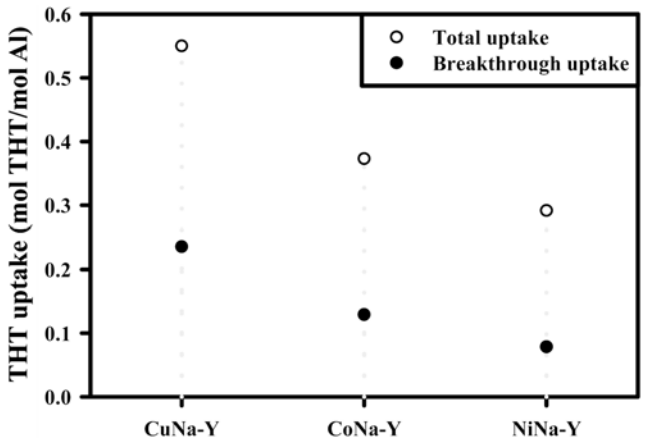

Fig. 3. The breakthrough uptake and the saturation uptake of THT on CuNa-Y, CoNa-Y, and NiNa-Y.

Table 2. Comparison of the breakthrough uptake of THT among various adsorbents

Adsorbent	Breakthrough capacity (mg of THT/g)	Reference
CuNa-Y	131.7	in this study
H-USY	79.0	[11]
3% Fe/BEA	127.7	[13]
16.7% $AgNO_3$/BEA	41.1	[14]
H-BEA	14.9	[15]
Na-Y	104.9	[22]
24.4% AgNa-Y	137.5	[22]
GaAl-Y	17.4	[26]

the THT could be detected in the effluent stream was dependent on the kinds of adsorbent and increased in the following order: NiNa-Y<CoNa-Y<CuNa-Y. The breakthrough uptake and the total uptake over these adsorbents were calculated and displayed in Fig. 3. For all data, the THT uptake was normalized based on the amount of structural aluminum to circumvent the effect of mass of each metal ion on the specific adsorption capacity (mol THT/g). The total uptake and the breakthrough uptake decreased in the following order: CuNa-Y>CoNa-Y>NiNa-Y. The total uptake is in line with the specific micropore volume. A comparison of the breakthrough uptake was made among different adsorbents as listed in Table 2. The breakthrough uptake of CuNa-Y was found to be a little lower than that of AgNa-Y. The lower price of these transition metals may compromise this lower uptake capacity. Anyway, it can be concluded that the THT uptake must be affected by the kind of metal ions in MNa-Y.

The interaction between THT and an adsorbent can be probed with the temperature-programmed desorption (TPD) technique after adsorption of THT on the adsorbent. These TPD patterns were obtained for four metal ion-exchanged Na-Y as shown in Fig. 4. As a reference, the TPD pattern for the parent Na-Y is also displayed. A major THT desorption peak appeared at ~470 K for Na-Y indicating strong adsorptive interactions between THT and the adsorption sites in Na-Y. A small peak also appeared at ~370 K due to desorption of the weakly adsorbed THT molecules. For CuNa-Y, rather

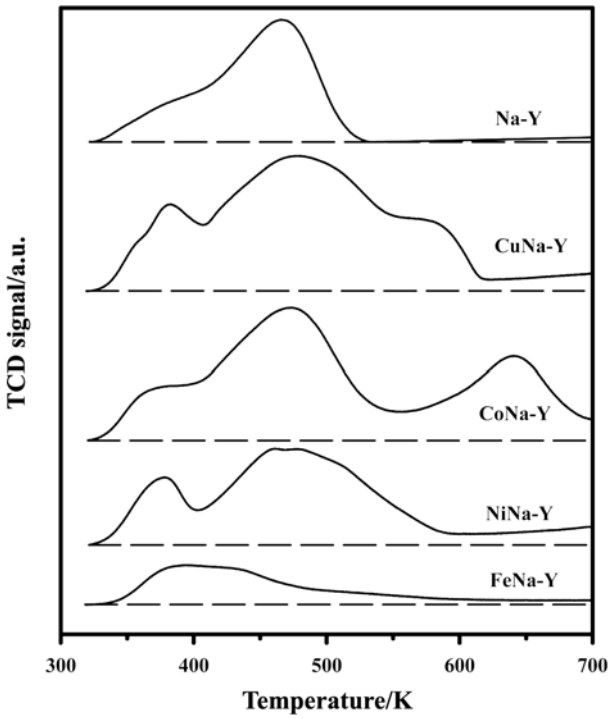

Fig. 4. Temperature-programmed desorption (TPD) patterns of THT adsorbed on FeNa-Y, NiNa-Y, CoNa-Y, CuNa-Y, and Na-Y.

broad TPD peaks can be found with maxima at ~380, ~480, and 580 K. A shoulder TPD peak at ~360 K also appeared. Two separate peaks can be observed over CoNa-Y in which the low-temperature TPD peak at ~470 K with a shoulder at ~360 K and the high-temperature TPD peak at ~640 K can be monitored. In the case of NiNa-Y, two adjacent TPD peaks with maxima at ~380 and ~480 K can be found at low temperatures. A much weaker broad TPD peak with maxima at ~390 and ~430 K was observed over FeNa-Y. In the previous work, we assigned the TPD peak at ~470 K to the desorption peak of THT from Na^+ in Na-Y [22]. Therefore, the high temperature peaks at ~580 K, ~640 K, and 480 K can be due to the desorption of THT from Cu^+, Co^{2+}, and Ni^{2+} in MNa-Y. It is generally accepted that a high temperature TPD peak means that there is a stronger interaction between an adsorbent and an adsorbate. However, this interpretation can be successfully made only when the adsorbate does not decompose during the TPD experiment. In the previous work, we found that some of the adsorbed THT was decomposed over AgNa-Y at high temperatures during the TPD experiment. Therefore, we also analyzed the effluent stream by mass spectroscopy.

For all mass data, four representative m/e values, such as 34, 41, 56, and 88, were selected and presented in Fig. 5. The presence of THT in the effluent stream can be confirmed by m/e=41 and m/e=88. Although m/e=56 can be observed from THT, its relative intensity appeared to be larger over MNa-Y than the theoretical value observed over H-Y or Na-Y. This implies that some of adsorbed

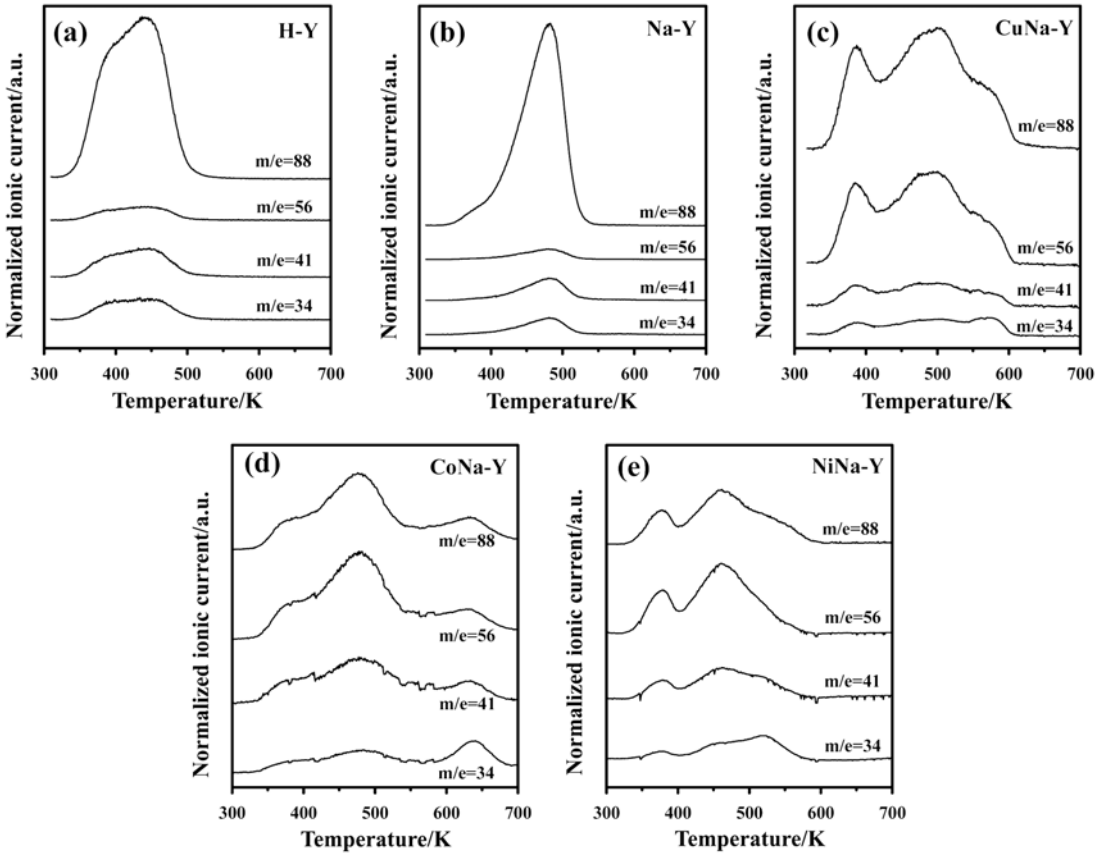

Fig. 5. The ionic current during temperature-programmed desorption (TPD) of THT adsorbed on H-Y (a), Na-Y (b), CuNa-Y (c), CoNa-Y (d), and NiNa-Y (e).

THT might be decomposed into C_4H_8 and H_2S in the presence of metal ions during TPD experiment. The decomposed products such as C_4H_8 and H_2S can be estimated with m/e=56 and m/e=34, respectively. For all mass data, the TPD profiles of m/e=41, 56, and 88 were identical to TPD patterns presented in Fig. 4. This result implies that the THT as well as C_4H_8 from THT evolves during the TPD experiment simultaneously. Some sites in MNa-Y must be responsible for the decomposition of THT. The peak position in the TPD profile of m/e=34 appeared to be similar to those of TPD patterns in Fig. 4. However, the relative peak intensities at different temperatures in the TPD profile of m/e=34 do not correspond to those of TPD pattern in Fig. 4. A larger peak intensity in the TPD profile of m/e=34 can be observed for all samples at high temperatures. This result implies that some H_2S formed at low temperatures desorbed at high temperatures. Based on the TPD patterns determined with the thermal conductive detector as well as the mass spectroscopy, the interaction between THT and metal ions in MNa-Y decreased in the following order: $Co^{2+}>Cu^{+}>Ni^{2+}$.

CONCLUSION

Among metal ion-exchanged MNa-Y such as CuNa-Y, CoNa-Y, NiNa-Y and FeNa-Y, CuNa-Y showed the largest breakthrough and total THT uptake. The total THT uptake is in line with the specific micropore volume. The interaction between THT and the metal ions decreased in the following order: $Co^{2+}>Cu^{+}>Ni^{2+}$. Some of THT were decomposed into C_4H_8 and H_2S over MNa-Y during the TPD experiment. C_4H_8 desorbed at the same temperature with THT, but some of H_2S still adsorbed at low temperatures and desorbed at high temperatures.

ACKNOWLEDGMENT

This work was supported by the Korea Research Foundation Grant funded by the Korean Government (MEST) (KRF-2007-412-J04001).

REFERENCES

1. C. Song, *Catal. Today*, **77**, 17 (2002).
2. R. Ferrauto, S. Hwang, L. Shore, W. Ruettinger, J. Lampert, T. Giroux, Y. Liu and O. Ilinich, *Annu. Rev. Mater. Res.*, **33**, 1 (2003).
3. R. T. Yang, A. J. Hernández-Maldonado and F. H. Yang, *Science*, **301**, 79 (2003).
4. X. Ma, L. Sun and C. Song, *Catal. Today*, **77**, 107 (2002).
5. A. L. Dicks, *J. Power Sources*, **61**, 113 (1996).
6. P. J. de Wild, R. G. Nyqvist, F. A. de Bruijn and E. R. Stobbe, *J. Power Sources*, **159**, 995 (2006).
7. S. Haji and C. Erkey, *Ind. Eng. Chem. Res.*, **42**, 6933 (2003).
8. P. Jeevanandam, K. J. Klabunde and S. H. Tetzler, *Micropor. Mesopor. Mater.*, **79**, 101 (2005).
9. A. B. S. H. Salem, *Ind. Eng. Chem. Res.*, **33**, 336 (1994).
10. A. B. S. H. Salem and H. S. Hamid, *Chem. Eng. Technol.*, **20**, 342 (1997).
11. I. Bezverkhyy, K. Bouguessa, C. Geantet and M. Vrinat, *Appl. Catal. B: Environ.*, **62**, 299 (2006).
12. C. L. Garcia and J. A. Lercher, *J. Phys. Chem.*, **95**, 10729 (1991).
13. H.-S. Roh, K.-W. Jun, J.-Y. Kim, J.-W. Kim, D.-R. Park, J.-D. Kim and S.-S. Yang, *J. Ind. Eng. Chem.*, **10**, 511 (2004).
14. H.-I. Song, C. H. Ko, J. C. Kim and J.-N. Kim, *Korean Chem. Eng. Res.*, **45**, 143 (2007).
15. S.-S. Oh and G-J. Kim, *J. Korean Ind. Eng. Chem.*, **18**, 459 (2007).
16. F. T. T. Ng, A. Rahman, T. Ohasi and M. Jiang, *Appl. Catal. B: Environ.*, **56**, 127 (2005).
17. A. J. Hernández-Maldonado and R. T. Yang, *AIChE J.*, **50**, 791 (2004).
18. S. Velu, X. Ma and C. Song, *Ind. Eng. Chem. Res.*, **42**, 5293 (2003).
19. M. Xue, R. Chitrakar, K. Sakane, T. Hirotsu, K. Ooi, Y. Yoshimura, Q. Feng and N. Sumida, *J. Colloid Interface Sci.*, **285**, 487 (2005).
20. K. Shimizu, N. Kobayashi, A. Satsuma, T. Kojima and S. Satokawa, *J. Phys. Chem. B*, **110**, 22570 (2006).
21. S. Satokawa, Y. Kobatashi and H. Fujiki, *Appl. Catal. B: Environ.*, **56**, 51 (2005).
22. D. Lee, E.-Y. Ko, H. C. Lee, S. Kim and E. D. Park, *Appl. Catal. A: Gen.*, **334**, 129 (2008).
23. S.-S. Oh and G-J. Kim, *J. Korean Ind. Eng. Chem.*, **18**, 337 (2007).
24. H. T. Kim, K.-W. Jun, H. S. Potdar, Y.-S. Yoon and M.-J. Kim, *Energy Fuels*, **21**, 327 (2007).
25. H. T. Kim, K.-W. Jun, S.-M. Kim, H. S. Potdar and Y.-S. Yoon, *Energy Fuels*, **20**, 2170 (2006).
26. K. Tang, L. Song, L. Duan, X. Li, J. Gui and Z. Sun, *Fuel Process. Technol.*, **89**, 1 (2008).
27. H. Cui, S. Q. Turn and M. A. Reese, *Energy Fuels*, **22**, 2550 (2008).
28. D. Lee, J. Kim, H. C. Lee, K. H. Lee, E. D. Park and H. C. Woo, *J. Phys. Chem. C*, **112**, 18955 (2008).
29. E. D. Park, S. H. Choi, D. Lee and H. C. Lee, *J. Nanosci. Nanotechnol. in press*.
30. B. C. Lippens and J. H. de Boer, *J. Catal.*, **4,** 319 (1965).
31. A. Takahashi, R. T. Yang, C. L. Munson and D. Chinn, *Ind. Eng. Chem. Res.*, **40**, 3979 (2001).
32. M. A. Keane, *Microporous Mater.*, **3**, 385 (1995).
33. J. S. Kim and M. A. Keane, *J. Colloid Interface Sci.*, **232**, 126 (2000).
34. M. A. Keane, *Microporous Mater.*, **3**, 93 (1994).
35. V. K. Kaushik and M. Ravindranathan, *Zeolites*, **12**, 415 (1992).
36. J. S. Kim, L. Zhang and M. A. Keane, *Sep. Sci. Technol.*, **36**, 1509 (2001).